Diagn Interv Radiol 2025; DOI: 10.4274/dir.2025.242880

ABDOMINAL IMAGING

ORIGINAL ARTICLE

Diffusion kurtosis versus diffusion-weighted magnetic resonance imaging in differentiating clear cell renal cell carcinoma and renal angiomyolipoma with minimal fat: a comparative study

Yarong Lin
Wenrong Zhu
Qingqiang Zhu

Department of Medical Imaging, Northern Jiangsu People's Hospital Affiliated to Yangzhou University, Yangzhou, China

PURPOSE

To quantitatively compare the diagnostic values of conventional diffusion-weighted imaging and diffusion kurtosis imaging (DKI) in differentiating clear cell renal cell carcinoma (ccRCC) and renal angiomyolipoma with minimal fat (RAMF).

METHODS

Sixty-eight patients with ccRCC and 18 patients with RAMF were retrospectively studied. For DKI and apparent diffusion coefficient (ADC), respiratory-triggered echo-planar imaging sequences were acquired in the axial plane (three *b*-values: 0, 1000, 2000 s/mm^2; one *b*-value: 2000 s/mm^2). Mean diffusivity (MD), fractional anisotropy (FA), mean kurtosis (MK), kurtosis anisotropy (KA), radial kurtosis (RK), and ADC were evaluated. The diagnostic efficacy of various diffusion parameters in predicting ccRCC and RAMF was compared.

RESULTS

The ADC and MD values of ccRCCs were higher than those of RAMFs ($P < 0.05$), whereas comparable FA, MK, and KA values were observed between ccRCCs and RAMFs ($P > 0.05$). Moreover, the RK values of RAMFs were higher than those of ccRCCs ($P < 0.05$). Receiver operating characteristic (ROC) curve analyses showed that MD values had the highest diagnostic efficacy in differentiating ccRCCs from RAMFs. In pairwise comparisons of ROC curves and diagnostic efficacy, DKI parameters demonstrated better diagnostic accuracy than ADC in differentiating between ccRCCs and RAMFs ($P < 0.05$).

CONCLUSION

DKI analysis demonstrates superior performance than ADC analysis in differentiating ccRCC and RAMF.

CLINICAL SIGNIFICANCE

DKI technology may serve as an additional non-invasive biomarker for the differential diagnosis of renal tumor types.

KEYWORDS

Kidney, renal cell carcinoma, diffusion kurtosis imaging, angiomyolipoma, differential diagnosis.

Corresponding author: Qingqiang Zhu

E-mail: zhuqingqiang1983@163.com

Received 04 June 2024; revision requested 21 July 2024; accepted 06 April 2025.

Epub: 21.07.2025

Publication date: 08.09.2025

DOI: 10.4274/dir.2025.242880

Clear cell renal cell carcinoma (ccRCC) is the predominant subtype of RCC, comprising approximately 70% of all RCC cases.[1] Angiomyolipomas that are predominantly composed of smooth muscle cells, those with a mixture of all three components (smooth muscle, fat, and blood vessels), or those exhibiting prominent cystic changes may be challenging to differentiate from epithelial neoplasms preoperatively.[2]

Renal angiomyolipoma with minimal fat (RAMF) is generally considered a benign lesion. In contrast, ccRCC is a malignant tumor with the potential for metastasis and life-threatening

You may cite this article as: Lin Y, Zhu W, Zhu Q. Diffusion kurtosis versus diffusion-weighted magnetic resonance imaging in differentiating clear cell renal cell carcinoma and renal angiomyolipoma with minimal fat: a comparative study. *Diagn Interv Radiol.* 2025;31(5):416-422.

consequences. The management strategies for RAMF and ccRCC may also differ substantially. For instance, RAMF, being benign, often allows for a biopsy followed by regular surveillance. However, ccRCC, given its malignant nature, typically necessitates surgical resection.

Advancements in imaging technology have substantially transformed the management of renal masses by enabling the detection and characterization of even very small lesions. However, conventional computed tomography (CT) and magnetic resonance imaging (MRI) still face limitations in distinguishing atypical malignant from benign lesions. Therefore, identifying a simple yet accurate method to differentiate renal carcinomas from benign lesions remains the critical objective of this study.

Apparent diffusion coefficient (ADC) assessment has also shown benefits in distinguishing renal tumor types. One meta-analysis of 17 studies demonstrated that ADC values can help differentiate benign from malignant RCC tumors.[3] However, there is ongoing concern that ADCs obtained from conventional monoexponential diffusion-weighted imaging (DWI) may not accurately reflect true diffusivity because of the influence of microcirculation.[4,5]

The diffusion kurtosis imaging (DKI) model, first described in 2005, is believed to provide a more complete mathematical representation of tissue microstructural complexity than the standard monoexponential model.[6-8] It attempts to account for diffusion variation and capture non-Gaussian diffusion behavior as a reflective marker of tissue heterogeneity.[9] The aim of the current study was to produce a quantitative comparison of the potential of various diffusion parameters obtained from DWI and DKI in differentiating ccRCC and RAMF.

Main points

- Diffusion kurtosis imaging parameters demonstrated better diagnostic accuracy than apparent diffusion coefficient (ADC) in differentiating between clear cell renal cell carcinomas (ccRCCs) and renal angiomyolipomas with minimal fat (RAMFs).
- The ADC and mean diffusivity values of ccRCCs were higher than those of RAMFs.
- The radial kurtosis values of RAMFs were higher than those of ccRCCs.

Methods

Participants

This retrospective study was approved by the institutional review committee of Northern Jiangsu People's Hospital Affiliated with Yangzhou University (protocol number: 20130701, date: 7/1/2013 to 9/1/2022), and the requirement for written informed consent was waived. The study covered the period from July 1, 2013, to September 1, 2022. A total of 117 adult patients who underwent routine MRI examinations and DKI assessment followed by partial or radical nephrectomy between July 2013 and September 2022 were retrospectively enrolled (Figure 1).

The exclusion criteria were as follows: (a) lesions without histopathological confirmation of ccRCC or RAMF (n = 13); (b) lesions requiring antiangiogenic therapy (n = 6); (c) tumor recurrence (n = 7); (d) a low signal-to-noise ratio (SNR) (n = 5; SNR <7.2 for b = 2000 s/mm^2). This retrospective study was approved by our institutional review board, with a waiver of the requirement for written informed consent.

Magnetic resonance imaging technique

MRI examinations were performed using a 3.0-T MR scanner (GE Signa EXCITE HD, Milwaukee, WI, USA) with a 6-channel array body coil and a 24-channel phased-array spine coil integrated into the scanner table. For DKI, a single-shot echo-planar imaging (EPI) sequence was applied in the axial plane using respiratory triggering via a respiratory belt, with three *b*-values (0, 1000, 2000 s/mm^2) and 30 diffusion directions. For ADC, respiratory-triggered EPI sequences were acquired in the axial plane (one *b*-value: 2000 s/mm^2). Other imaging parameters were as follows: 24 axial slices covering both kidneys; echo time: 73.9 ms; repetition time: 5000 ms; number of excitations: 4; matrix: 192 × 192; field of view: 400 mm. Array spatial sensitivity encoding technique, a parallel imaging method, was applied with an acceleration factor of 4.

Imaging analysis and statistics

The acquired images were transferred to an offline workstation for processing using Automated Image Registration software, version 4.6.4. (GE Signa EXCİTE HD, GE Healthcare, Milwaukee, WI, USA). Prior to the quantification of DKI and ADC, non-rigid co-registration and smoothing were performed using a 3 × 3 kernel matrix. All DWIs were first co-registered to the b0 image using the affine model. Then, registered DWIs with *b*-values of 1000 and 2000 s/mm^2 and ADCs with a *b*-value of 2000 s/mm^2 were averaged over 30 diffusion-encoding directions.

Afterward, the two averaged DWIs were co-registered to the b0 image using the affine model, and the registered averaged DWIs were set as a reference volume for further registrations. Finally, the initial DWIs with a *b*-value of 2000 s/mm^2 were co-registered to the corresponding reference volume using a non-rigid model. The registered DWIs were then spatially smoothed using a Gaussian filter with a full width at half-maximum of 2 mm. With our DKI and ADC protocol, we obtained parametric maps related to diffusional kurtosis: mean diffusivity (MD), fractional anisotropy (FA), mean kurtosis (MK), kurtosis anisotropy (KA), radial kurtosis (RK), and ADC. The assessment of renal tumors and region-of-interest (ROI) positioning was

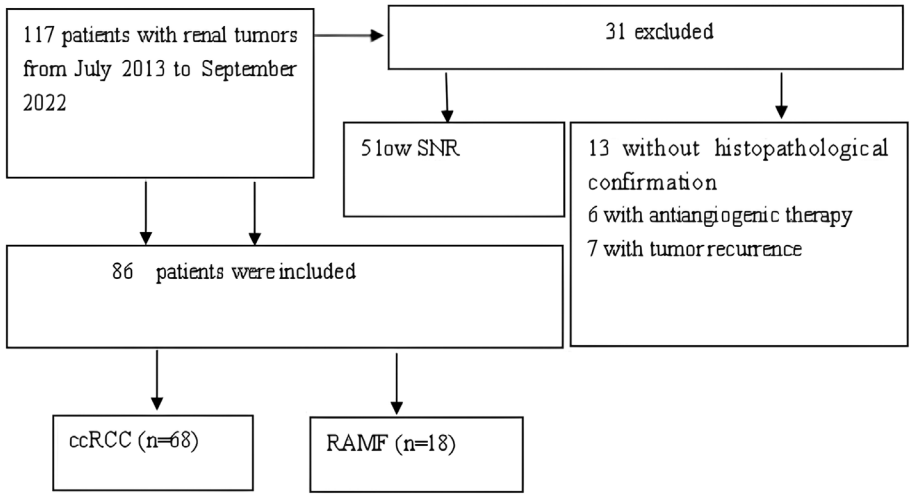

Figure 1. Patient inclusion and exclusion flowchart. SNR, signal-to-noise ratio; ccRCC, clear cell renal cell carcinoma; RAMF, renal angiomyolipoma with minimal fat.

conducted by two radiologists with 5 and 10 years of clinical experience in interpreting MRI, respectively. Both observers were blinded to the patients' clinical information and tumor histology. Lesion location, the number of layers on which the tumor appeared most prominent across different sequences, imaging characteristics of the renal tumors, and the ROI plotting method were considered.

The two observers, each with 5 and 10 years of diagnostic experience, analyzed all the parameter maps in conjunction with the DKI and ADC images. They were blinded to the pathologic diagnosis and reached a consensus on their analysis.

Free-hand ROIs were delineated around the most solid portion of each tumor (covering approximately two-thirds of the solid area) on the DKI and ADC maps. This was performed on three to five representative slices by the same two radiologists using ImageJ software (National Institutes of Health, Bethesda, MD, USA). The region with lower T2 signal intensity was identified as the most solid part in heterogeneous tumors. Strong hyperintensity on T2WI or T1WI indicated tissue necrosis or hemorrhage, and such regions were excluded. Mean values for ADC, MD, FA, MK, KA, and RK for each ROI were calculated using ImageJ software. The readers independently assessed images derived from the DKI and ADC examinations during two separate sessions, with an interval of more than four weeks between sessions to mitigate potential recall bias.

Statistical analysis

Statistical analysis was conducted using SPSS version 23.0 statistical software (SPSS, Chicago, IL, USA). Numeric data were expressed as means and standard deviations (±), and categorical data were expressed as percentages. Evaluated DKI and ADC features were compared between ccRCC and RAMF using the independent-sample t-test. A P value <0.05 was considered statistically significant.

To assess the diagnostic performance of DKI and ADC parameters in differentiating ccRCC from RAMF, we calculated the diagnostic accuracy for both tumor types. The highest Youden index value was used to determine the optimal diagnostic point, and the DeLong method[10] was applied to compare area under the curves. Intraclass correlation coefficients (ICCs) were used to assess interobserver agreement for ADC and DKI parameter measurements, with 95% confidence intervals (CIs). ICCs were interpreted as follows: ≤ 0.20, slight; 0.21–0.40, fair; 0.41–0.60, moderate; 0.61–0.80, substantial; and 0.81–1.00, perfect agreement.

The comparison of ICCs between observers with 5 and 10 years of experience was performed using a self-lifting resampling technique with 200 repetitions. This method was employed to estimate the mean ICC and 95% CI for each observer group. Retest reliability was calculated for individual observers as well as for the entire group, and comparisons were made using the Z-test for ICC. A P value <0.05 was considered statistically significant.

Results

Population demographics

A total of 86 patients with pathologically confirmed ccRCC and RAMF were included, comprising 68 patients (38 men and 30 women) with ccRCC and 18 patients (12 men and 6 women) with RAMF. The mean age at diagnosis was slightly lower in patients with RAMF (49.8 years; range 39 to 62 years) than in those with ccRCC (52.1 years; range 36 to 76 years). There was no difference in clinical manifestations between ccRCC and RAMF, such as mean age, sex, flank pain, palpable mass, and fever (all $P > 0.05$), except for hematuria (73 vs. 2, $P < 0.01$).

Apparent diffusion coefficient and diffusion kurtosis imaging parameters of the renal tumors

The ADC (Figure 2, Table 1) and MD (Figure 3, Table 1) values of ccRCCs were higher than those of RAMFs ($P < 0.05$). The RK (Figure 4) values of RAMFs were higher than those of ccRCCs (Figure 5, $P < 0.05$), whereas comparable FA, MK, and KA values were found between ccRCCs and RAMFs (Figure 6, Table 1; $P > 0.05$).

Diagnostic performance of multiple parameters

Receiver operating characteristic (ROC) curve analyses showed that MD (Figure 7, Table 2) and RK (Figure 8, Table 2) values had higher diagnostic efficacy than ADC values in differentiating ccRCCs from RAMFs. MD values demonstrated the highest diagnostic efficacy. For pairwise comparisons of ROC curves and diagnostic performance, ADC was inferior to MD and KA ($P < 0.05$).

The agreement of diffusion parameters in the 86 cases, both for individual observers and overall, was perfect for all parameters (ADC, MD, FA, MK, KA, and RK). Retest reliability, assessed by an independent repeat evaluation by two observers with 5 and 10 years of experience, was shown to be excellent (Table 3). In addition, there was no statistically significant difference in retest reliability between the two observers (Table 4).

Discussion

The ADC and MD values of ccRCCs were higher than those of RAMFs ($P < 0.05$), whereas comparable FA, MK, and KA values were found between ccRCCs and RAMFs ($P > 0.05$). Moreover, the RK values of RAMFs were

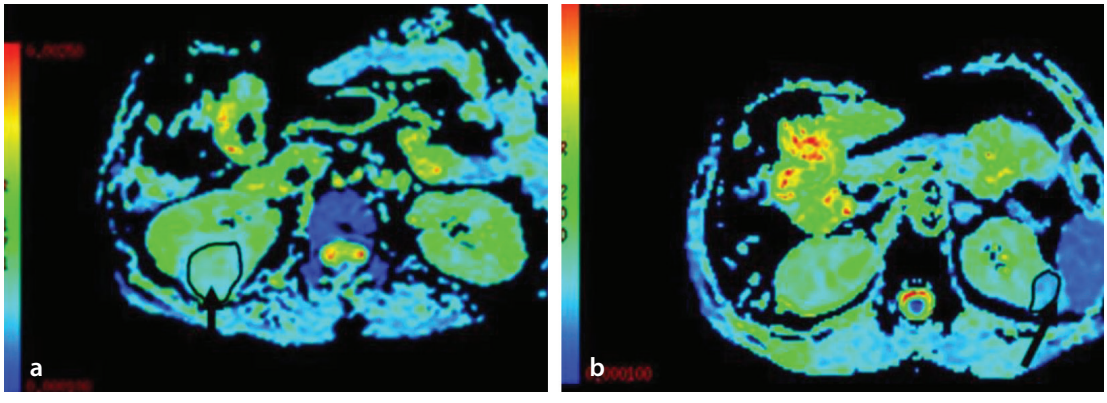

Figure 2. Apparent diffusion coefficient (ADC) features of clear cell renal cell carcinoma (ccRCC) **(a)** and renal angiomyolipoma with minimal fat (RAMF) **(b)**; ADC values were higher for ccRCC (0.89) and lower for RAMF (0.53).

Table 1. Diffusion kurtosis imaging and apparent diffusion coefficient parameters in clear cell renal cell carcinoma and renal angiomyolipoma with minimal fat

Parameters	ccRCC	RAMF	*P* values
ADC	0.81 ± 0.11	0.55 ± 0.18	<0.05
MD	2.13 ± 0.42	1.21 ± 0.26	<0.01
FA	0.17 ± 0.05	0.18 ± 0.04	>0.05
MK	0.92 ± 0.21	0.87 ± 0.16	>0.05
KA	0.99 ± 0.23	0.88 ± 0.19	>0.05
RK	0.66 ± 0.08	0.91 ± 0.24	<0.05

ccRCC, clear cell renal cell carcinoma; RAMF, renal angiomyolipoma with minimal fat; ADC, apparent diffusion coefficient; MD, mean diffusivity; FA, fractional anisotropy; MK, mean kurtosis; KA, kurtosis anisotropy; RK, radial kurtosis.

Table 2. Diagnostic test characteristics of diffusion parameters in differentiating clear cell renal cell carcinoma from renal angiomyolipoma with minimal fat

Parameters	AUC (95% CI)	Cut-off value	Sensitivity	Specificity	Accuracy
ccRCC (n = 68) vs. RAMF (n = 18)					
ADC ($\times 10^{-3}$ mm^2/s)	0.810 (0.821–0.933)	≥0.72	79.4% (54/68)	66.7% (12/18)	79.1% (68/86)
MD	0.943 (0.889–0.991)	≥1.83	94.1% (64/68)	83.3% (15/18)	94.2% (81/86)
RK	0.863 (0.808–0.921)	≤0.68	86.7% (59/68)	77.8% (14/18)	84.9% (73/86)

AUC, area under the curve; ccRCC, clear cell renal cell carcinoma; RAMF, renal angiomyolipoma with minimal fat; ADC, apparent diffusion coefficient; MD, mean diffusivity; RK, radial kurtosis.

Table 3. Intraclass correlation coefficients for measurements of apparent diffusion coefficient, mean diffusivity, fractional anisotropy, mean kurtosis, kurtosis anisotropy, and radial kurtosis by total observers

Parameters	Observer ICC
ADC	0.931 (0.911–0.952)
MD	0.951 (0.929–0.991)
FA	0.893 (0.871–0.911)
MK	0.916 (0.911–0.949)
KA	0.926 (0.901–0.963)
RK	0.911 (0.901–0.936)

ADC, apparent diffusion coefficient; MD, mean diffusivity; FA, fractional anisotropy; MK, mean kurtosis; KA, kurtosis anisotropy; RK, radial kurtosis; ICC, Intraclass correlation coefficient.

Table 4. Intraclass correlation coefficients for measurements of apparent diffusion coefficient, mean diffusivity, fractional anisotropy, mean kurtosis, kurtosis anisotropy, and radial kurtosis by individual observers

Parameters	Individual observer (first vs. second)	*P* values
ADC	0.903 (0.881–0.923) vs. 0.933 (0.907–0.968)	>0.05
MD	0.933 (0.907–0.963) vs. 0.947 (0.913–0.963)	>0.05
FA	0.886 (0.863–0.902) vs. 0.906 (0.882–0.922)	>0.05
MK	0.893 (0.886–0.921) vs. 0.921 (0.912–0.952)	>0.05
KA	0.907 (0.886–0.938) vs. 0.931 (0.912–0.966)	>0.05
RK	0.901 (0.883–0.926) vs. 0.923 (0.911–0.946)	>0.05

ADC, apparent diffusion coefficient; MD, mean diffusivity; FA, fractional anisotropy; MK, mean kurtosis; KA, kurtosis anisotropy; RK, radial kurtosis.

higher than those of ccRCCs ($P < 0.05$). ROC curve analyses showed that MD values had the highest diagnostic efficacy in differentiating ccRCCs from RAMFs. For pairwise comparisons of ROC curves and diagnostic efficacy, ADC was inferior to DKI analysis ($P < 0.05$).

DKI is a dimensionless measure that quantifies the deviation of the water diffusion displacement profile from the Gaussian distribution of unrestricted diffusion, providing a measure of the degree of diffusion hindrance or restriction.[11] It has been shown to offer superior sensitivity over conventional DTI.[12] An appealing aspect of incorporating DKI into routine clinical practice is that it can be performed in a straightforward manner, as the sequence is performed in essentially the same manner as a standard DWI sequence,[13] aside from the generally higher *b*-values required.

In a recent study, Lanzman et al.[14] highlighted the potential of DTI for non-invasive functional assessment of transplanted kidneys. They also demonstrated significant differences in FA values of the medulla between

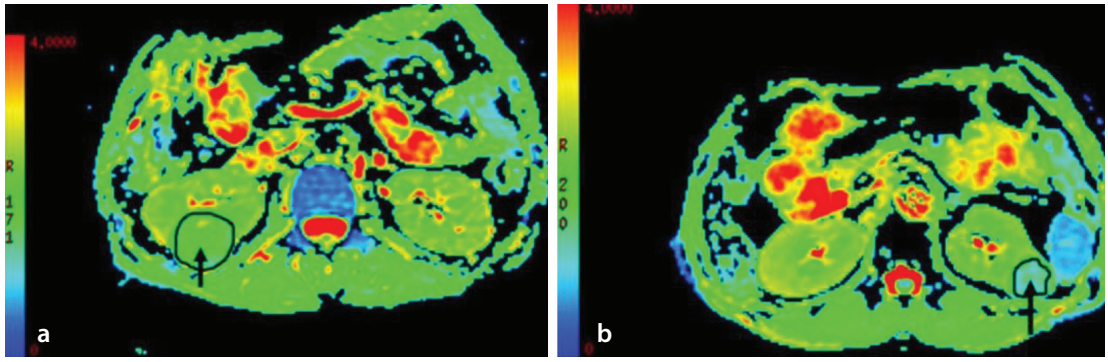

Figure 3. Mean diffusivity (MD) features of clear cell renal cell carcinoma (ccRCC) **(a)** and renal angiomyolipoma with minimal fat (RAMF) **(b)**; MD values were higher for ccRCC (2.17) and lower for RAMF (1.42).

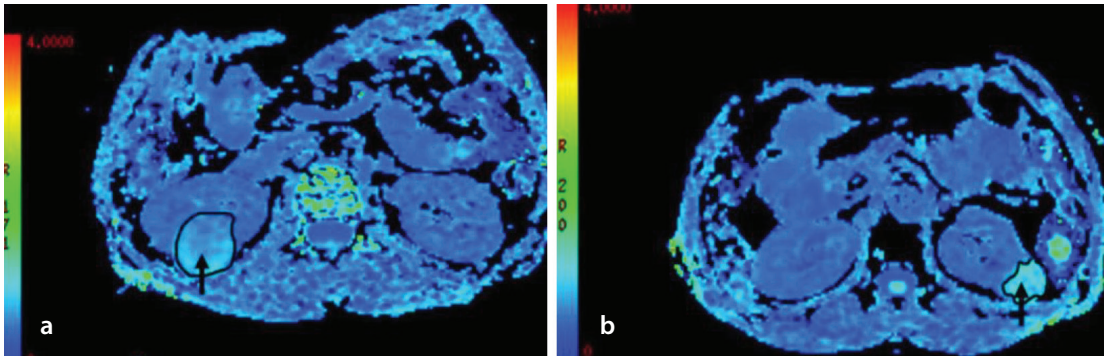

Figure 4. Radial kurtosis (RK) features of clear cell renal cell carcinoma (ccRCC) **(a)** and renal angiomyolipoma with minimal fat (RAMF) **(b)**; RK values were lower for ccRCC (0.71) and higher for RAMF (0.97).

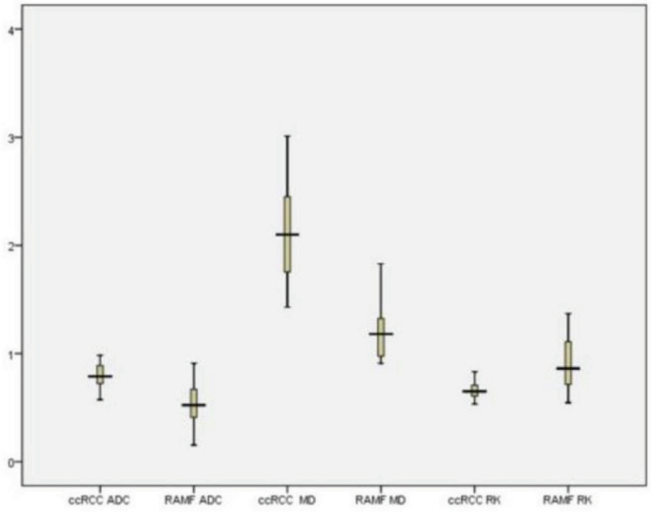

Figure 5. Box-and-whisker plots showing the distribution of apparent diffusion coefficient, mean diffusivity, and radial kurtosis parameters, with significant differences between clear cell renal cell carcinoma and renal angiomyolipoma with minimal fat. ccRCC, clear cell renal cell carcinoma; RAMF, renal angiomyolipoma with minimal fat; ADC, apparent diffusion coefficient; MD, mean diffusivity; RK, radial kurtosis.

allograft recipients with severely impaired renal function and those with moderate or mild impairment. Comparing MK values of normal kidneys with those of patients with various renal diseases may help evaluate the clinical significance of renal kurtosis values and the role of renal DKI.[15] For instance, in RCC, DKI may provide additional diagnostic information. Since DKI has been proven to be more sensitive to tissue microstructure than FA measures, DKI of the kidney might be useful in evaluating conditions involving renal tumors.[16] Notohamiprodjo et al.[17] reported that higher *b*-values and a greater number of directions improve the accuracy of diffusion measurements. In our study, we demonstrated that *b*-values in the range of 0 to 2000 s/mm^2 with 30 diffusion-encoding directions are sufficient in abdominal DKI to observe the departure of the diffusion signal from monoexponential behavior.

In our study, statistically significant differences were observed in the MD and ADC values between ccRCC and RAMF. Many authors attribute higher MD and ADC to higher cellularity. Tissue-free water content and structural differences can influence MD and ADC. Increases in MD and ADC due to micronecrosis or altered viscosity of the medium may counterbalance decreased MD and ADC values in ccRCC.[18] ccRCC is rich in lipid content; cholesterol, neutral lipids, and phospholipids are abundant in pathology.[19]

An increase in the number of cells or a decrease in cell volume leads to an increase in the diffusion limitation of water molecules, which results in an increase in RK.[20] Necrotic areas within the tumor and surrounding edema change the diffusion characteristics, usually with lower RK values in the necrotic areas and higher RK values in the edematous areas. As illustrated in our study, RAMF showed greater RK values than ccRCC, with a significant difference consistent with the understanding that RAMF has greater viscosity and restricted water diffusion due to the presence of hemorrhagic walls or hemosiderin deposition.

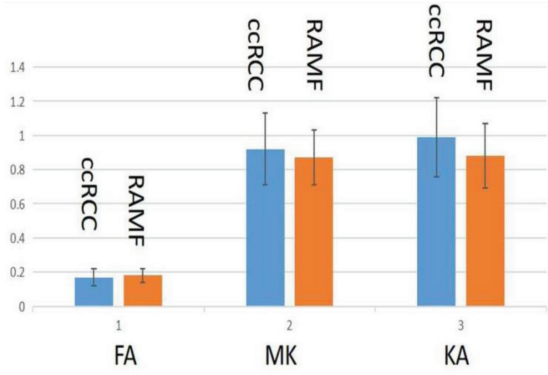

Figure 6. Bar graph showing the distribution of fractional anisotropy, mean kurtosis, and kurtosis anisotropy parameters, without significant differences between clear cell renal cell carcinoma and renal angiomyolipoma with minimal fat. ccRCC, clear cell renal cell carcinoma; RAMF, renal angiomyolipoma with minimal fat; FA, fractional anisotropy; MK, mean kurtosis; KA, kurtosis anisotropy.

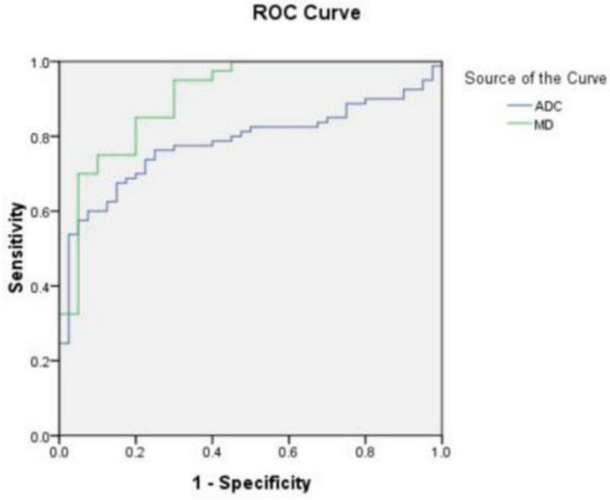

Figure 7. Receiver operating characteristic curves showing the diagnostic performance of apparent diffusion coefficient and mean diffusivity parameters in differentiating clear cell renal cell carcinoma from renal angiomyolipoma with minimal fat. ROC, receiver operating characteristic; ADC, apparent diffusion coefficient; MD, mean diffusivity.

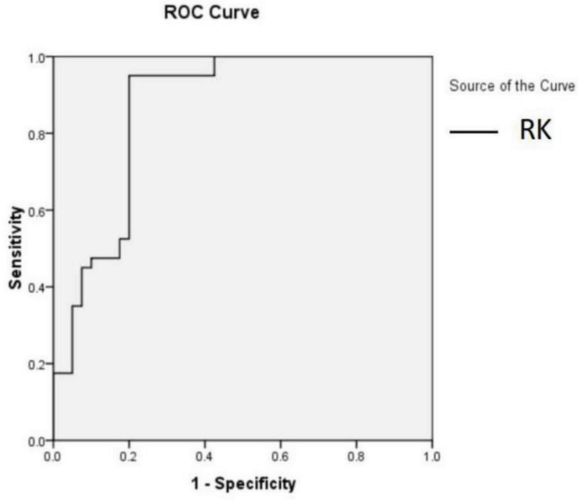

Figure 8. Receiver operating characteristic curves showing the diagnostic performance of radial kurtosis in differentiating clear cell renal cell carcinoma from renal angiomyolipoma with minimal fat. ROC, receiver operating characteristic; RK, radial kurtosis.

The MD and RK parameters showed greater discrimination of renal tumor types than the ADC parameters, perhaps because the latter includes both microcirculation and tissue cellularity information.[21] These two sources of information may affect the ADC measurement in opposing ways, decreasing sensitivity and specificity.[22] Moreover, the additional MD and RK parameters provide specific information on non-Gaussian diffusion behavior, offering a more accurate measurement of tissue diffusion.[23]

Retest reliability was evaluated through an independent repeat assessment conducted by two observers with 5 and 10 years of experience, respectively. The results demonstrated excellent retest reliability. Furthermore, no statistically significant difference in retest reliability was observed between the two observers. This finding suggests that the stability of DKI in evaluating microstructural differences in ccRCC and RAMF is not influenced by the observers' level of experience. Such consistency is highly conducive to the clinical adoption and broader application of DKI technology.

The main limitation of our study is the small number of patients in each renal tumor type, especially RAMF. Further studies with larger populations are recommended to validate our findings. We acknowledge additional limitations in the current study. As a single-center, retrospective analysis, the findings may be influenced by the specific characteristics of the sample population and the inherent biases associated with retrospective data collection. Therefore, the reliability of our results should be confirmed through well-designed prospective studies and multicenter investigations.

Notably, our study did not include comparisons with other subtypes of RCC or with renal oncocytomas. As a result, it would be overly speculative to extrapolate our findings to differentiate renal oncocytomas from other types of renal tumors. However, papillary and chromophobe RCCs, as well as renal oncocytomas, are generally less likely to be confused with ccRCC or RAMF on CT and/or MRI. ccRCC and RAMF typically exhibit hypervascularity and heterogeneous enhancement, whereas papillary and chromophobe RCCs are characterized by hypovascularity. In contrast, renal oncocytomas are often identified by a central stellate scar, homogeneous enhancement, and a spoke-wheel pattern of enhancement, which are considered characteristic features.

In conclusion, DKI parameters demonstrated better performance than ADC in differentiating ccRCC and RAMF. This new technique can potentially be used as another non-invasive biomarker for the differential diagnosis of renal tumor types.

Footnotes

Conflict of interest disclosure

The authors declared no conflicts of interest.

References

1. Jomoto W, Takaki H, Yamamoto S, et al. Differentiation of angiomyolipoma with minimal fat from clear cell renal cell carcinoma using non-contrast multiparametric magnetic resonance imaging. *In Vivo*. 2022;36(6):2790-2799. [Crossref]
2. Li H, Li A, Zhu H, et al. Whole-tumor quantitative apparent diffusion coefficient histogram and texture analysis to differentiation of minimal fat angiomyolipoma from clear cell renal cell carcinoma. *Acad Radiol*. 2019;26(5):632-639. [Crossref]
3. Lassel EA, Rao R, Schwenke C, Schoenberg SO, Michaely HJ. Diffusion-weighted imaging of focal renal lesions: a meta-analysis. *Eur Radiol*. 2014;24(1):241-249. [Crossref]
4. Cao J, Luo X, Zhou Z, et al. Comparison of diffusion-weighted imaging mono-exponential mode with diffusion kurtosis imaging for predicting pathological grades of clear cell renal cell carcinoma. *Eur J Radiol*. 2020;130:109195. [Crossref]
5. Parada Villavicencio C, Mc Carthy RJ, Miller FH. Can diffusion-weighted magnetic resonance imaging of clear cell renal carcinoma predict low from high nuclear grade tumors. *Abdom Radiol (NY)*. 2017;42(4):1241-1249. [Crossref]
6. Zhang J, Suo S, Liu G, et al. Comparison of monoexponential, biexponential, stretched-exponential, and kurtosis models of diffusion-weighted imaging in differentiation of renal solid masses. *Korean J Radiol*. 2019;20(5):791-800. [Crossref]
7. Fu J, Ye J, Zhu W, Wu J, Chen W, Zhu Q. Magnetic resonance diffusion kurtosis imaging in differential diagnosis of benign and malignant renal tumors. *Cancer Imaging*. 2021;21(1):6. [Crossref]
8. Cheng ZY, Feng YZ, Liu XL, Ye YJ, Hu JJ, Cai XR. Diffusional kurtosis imaging of kidneys in patients with hyperuricemia: initial study. *Acta Radiol*. 2020;61(6):839-847. [Crossref]
9. Novello L, Henriques RN, Ianuş A, Feiweier T, Shemesh N, Jovicich J. In vivo correlation tensor MRI reveals microscopic kurtosis in the human brain on a clinical 3T scanner. *Neuroimage*. 2022;254:119137. [Crossref]
10. DeLong ER, DeLong DM, Clarke-Pearson DL. Comparing the areas under two or more correlated receiver operating characteristic curves: a nonparametric approach. *Biometrics*. 1988;44(3):837-845. [Crossref]
11. Wu G, Zhao Z, Yao Q, et al. The study of clear cell renal cell carcinoma with MR diffusion kurtosis tensor imaging and its histopathologic correlation. *Acad Radiol*. 2018;25(4):430-438. [Crossref].
12. DiBella EVR, Sharma A, Richards L, Prabhakaran V, Majersik JJ, HashemizadehKolowri SK. Beyond diffusion tensor MRI methods for improved characterization of the brain after ischemic stroke: a review. *AJNR Am J Neuroradiol*. 2022;43(5):661-669. [Crossref]
13. Zhu J, Luo X, Gao J, Li S, Li C, Chen M. Application of diffusion kurtosis tensor MR imaging in characterization of renal cell carcinomas with different pathological types and grades. *Cancer Imaging*. 2021;21(1):30. [Crossref]
14. Lanzman RS, Ljimani A, Pentang G, et al. Kidney transplant: functional assessment with diffusion-tensor MR imaging at 3T. *Radiology*. 2013;266(1):218-225. [Crossref]
15. Dai Y, Yao Q, Wu G, et al. Characterization of clear cell renal cell carcinoma with diffusion kurtosis imaging: correlation between diffusion kurtosis parameters and tumor cellularity. *NMR Biomed*. 2016;29(7):873-881. [Crossref]
16. Ding Y, Tan Q, Mao W, et al. Differentiating between malignant and benign renal tumors: do IVIM and diffusion kurtosis imaging perform better than DWI? *Eur Radiol*. 2019;29(12):6930-6939. [Crossref]
17. Notohamiprodjo M, Dietrich O, Horger W, et al. Diffusion tensor imaging (DTI) of the kidney at 3 tesla-feasibility, protocol evaluation and comparison to 1.5 Tesla. *Invest Radiol*. 2010;45(5):245-254. [Crossref]
18. Minervini A, Di Cristofano C, Gacci M, et al. Prognostic role of histological necrosis for nonmetastatic clear cell renal cell carcinoma: correlation with pathological features and molecular markers. *J Urol*. 2008;180(4):1284-1289. [Crossref]
19. Koh MJ, Lim BJ, Choi KH, Kim YH, Jeong HJ. Renal histologic parameters influencing postoperative renal function in renal cell carcinoma patients. *Korean J Pathol*. 2013;47(6):557-562. [Crossref]
20. Huang Y, Chen X, Zhang Z, et al. MRI quantification of non-Gaussian water diffusion in normal human kidney: a diffusional kurtosis imaging study. *NMR Biomed*. 2015;28(2):154-161. [Crossref]
21. Zhang YD, Wu CJ, Wang Q, et al. Comparison of Utility of Histogram Apparent Diffusion Coefficient and R2* for differentiation of low-grade from high-grade clear cell renal cell carcinoma. *AJR Am J Roentgenol*. 2015;205(2):W193-201. [Crossref]
22. Reynolds HM, Parameswaran BK, Finnegan ME, et al. Diffusion weighted and dynamic contrast enhanced MRI as an imaging biomarker for stereotactic ablative body radiotherapy (SABR) of primary renal cell carcinoma. *PLoS One*. 2018;13(8):e0202387. [Crossref]
23. Ding Y, Zeng M, Rao S, Chen C, Fu C, Zhou J. Comparison of biexponential and monoexponential model of diffusion-weighted imaging for distinguishing between common renal cell carcinoma and fat poor angiomyolipoma. *Korean J Radiol*. 2016;17(6):853-863. [Crossref]